*J. Fluid Mech.* (2007), *vol.* 582, *pp.* 463–472.  
doi:10.1017/S0022112007006507 Printed in the United Kingdom

# Influence of crest and group length on the occurrence of freak waves

ODIN GRAMSTAD AND KARSTEN TRULSEN
Department of Mathematics, University of Oslo, P.O. Box 1053 Blindern, NO-0316 Oslo, Norway

(Received 18 December 2006 and in revised form 17 April 2007)

A large number of simulations have been performed to reveal how the occurrence of freak waves on deep water depends on the group and crest lengths for fixed steepness. It is found that there is a sharp qualitative transition between short- and long-crested sea, for a crest length of approximately ten wavelengths. For short crest lengths the statistics of freak waves deviates little from Gaussian and their occurrence is independent of group length (or Benjamin–Feir index, BFI). For long crest lengths the statistics of freak waves is strongly non-Gaussian and the group length (or BFI) is a good indicator of increased freak wave activity.

## 1. Introduction

Standard linear theory for the sea surface predicts Gaussian wave statistics, while it is commonly found that the surface of a deep sea is slightly non-Gaussian. Well-known deterministic mechanisms explain how freak waves may be provoked in special circumstances such as refraction of waves due to currents or bathymetry and dispersive focusing in space or time, in one or two horizontal dimensions. However, our concern here are freak waves occurring naturally in open sea in the absence of currents and topography.

From weakly nonlinear narrow-band theory, it is common to distinguish two reasons why the statistics of the sea surface can deviate from Gaussian. We will assume that the wave field can be decomposed into a superposition of free waves that satisfy the dispersion relation, and nonlinearly bound waves that do not satisfy the dispersion relation. The non-free waves are phase-locked to the free waves. In the standard linear theory the free waves are assumed to yield Gaussian statistics. The nonlinearly bound waves produce small corrections to Gaussian statistics, known as Tayfun distributions (Tayfun 1980). On the other hand, the free waves evolve owing to nonlinear interactions. It has been anticipated that the nonlinear evolution of the free waves can produce increased occurrence of freak waves, and significant deviation from Gaussian statistics.

Modulational instabilities such as the Benjamin–Feir instability (Benjamin 1967; McLean *et al.* 1981) are traditionally suspected prime candidates for freak wave production. So-called 'breathers' are extreme waves provoked by Benjamin–Feir instability such that a uniform wavetrain develops into a few extreme waves and then relaxes back to a uniform wavetrain (Dysthe & Trulsen 1999; Osborne, Onorato & Serio 2000). Similar mechanisms have been demonstrated numerically for long-crested waves (Clamond & Grue 2002), and have been suggested theoretically for crossing sea states (Onorato, Osborne & Serio 2006).

When the background spectrum becomes broad, modulational instability of the Benjamin–Feir type is reduced and eventually vanishes. This stabilization is known to depend on the ratio of steepness to bandwidth. Alber (1978) first derived this result for a Gaussian wave vector spectrum with equal bandwidths in both horizontal directions. Crawford, Saffman & Yuen (1980) looked at a Cauchy wave vector spectrum and showed that the stabilization only depends on the bandwidth of the wave vector component in the main propagation direction, and does not depend on the transversal direction (crest length). They found that a narrow-banded wave field can experience modulational instabilities when the ratio $2\epsilon k_p/\Delta k_x$ is larger than one, where $\epsilon$ is the average wave steepness and $\Delta k_x$ is the spectral bandwidth in the direction of the main wave propagation and $k_p$ is the peak wavenumber. Recently, the ratio of steepness to bandwidth has become known as the Benjamin–Feir index (BFI) following Janssen (2003), who defined it in terms of frequency bandwidth as

$$\mathrm{BFI} = \frac{\epsilon}{\Delta\omega/\omega_p}, \tag{1.1}$$

where $\Delta\omega$ and $\omega_p$ are respectively the bandwidth and the peak frequency in the frequency spectrum. This ratio was previously called an 'Ursell number' by Onorato *et al.* (2001). The BFI is usually normalized such that a random wavetrain is unstable if $\mathrm{BFI} > 1$. BFI has been suggested as an indicator for the probability of occurrence of freak waves in the sense that large BFI means larger probability of freak waves.

For long-crested waves there is both numerical and experimental evidence that freak wave activity increases when BFI is large. Onorato *et al.* (2001) searched for freak waves in a long-crested sea initialized with a JONSWAP spectrum that evolves according to the cubic nonlinear Schrödinger equation. They found that the probability of freak waves increases with both the spectral peak enhancement coefficient and the overall steepness of the spectrum. Janssen (2003) reported a correlation between BFI and freak wave activity in numerical simulations of long-crested deep-water waves using the Zakharov integral equation. Onorato *et al.* (2004) reported experimental observations of wave statistics for long-crested waves initialized with a JONSWAP spectrum in a long flume. They observed that for large values of BFI the kurtosis of the surface elevation was significantly greater than 3 and more extreme waves occurred than predicted by the Rayleigh distribution. For small values of BFI the statistics was closer to Gaussian. Later, Onorato, Osborne & Serio (2005*a*) provided numerical evidence that modulational instability was responsible for the increased freak wave activity in those experiments.

For short-crested waves there is both numerical and experimental evidence that freak wave activity decreases when the crest length is short. Stansberg (1994) reported experiments with long- and short-crested waves and noted that the nonlinear modulation of wave groups essentially disappears for short crest lengths. He also reported that wave statistics for long-crested waves deviates from Gaussian toward more freak waves, while wave statistics for short-crested waves is essentially Gaussian. Onorato, Osborne & Serio (2002) reported numerical simulations using a modified nonlinear Schrödinger equation where the number of extreme wave events was reduced when the directionality of the initial spectrum was increased. Socquet-Juglard *et al.* (2005) reported numerical results using a modified nonlinear Schrödinger equation. For short crest lengths they found deviation from Gaussian statistics only due to bound nonlinear contributions to the wave field, while free waves preserve Gaussian statistics despite third-order nonlinear evolution. The statistics of the numerically simulated sea surface thus showed excellent agreement with Tayfun

distributions. For long-crested seas they found that free waves do deviate from Gaussian statistics due to the nonlinear evolution. Waseda (2006) reported wave tank experiments using directional JONSWAP spectra. He found that the occurrence of extreme waves is significantly reduced when the directionality broadens.

As BFI does not contain information about the crest length we anticipate that it alone is not a good parameter for predicting the probability of freak waves. Our main purpose is to investigate how the occurrence of freak waves simultaneously depends on BFI and the crest length. Given a wave vector spectrum with peak $\boldsymbol{k}_p = (k_p, 0)$ and bandwidths $\Delta k_x$ and $\Delta k_y$, we define the crest length, $L_c$, as

$$L_c = \frac{k_p}{\Delta k_y}. \tag{1.2}$$

A positive correlation is anticipated between the kurtosis and the probability of freak waves. Mori & Janssen (2006) showed such a correlation using Edgeworth distributions, and gave field evidence of directional wave fields supporting this result. We give numerical evidence for the same correlation below.

Recently, a relationship between BFI and kurtosis has also been suggested by Janssen (2003), Onorato, Osborne & Serio (2005*b*) and Mori & Janssen (2006). They showed that the kurtosis of the sea surface depends on three contributions: a Gaussian contribution equal to 3, a nonlinear bound-wave contribution proportional to the steepness squared and a nonlinear free-wave contribution which in the limit of long time is shown to be proportional to BFI squared. For the relatively narrow bandwidths we are concerned with here, the free-wave contribution dominates the bound-wave contribution. BFI can be computed from the spectrum alone, and can thus be derived from a conventional spectral wave forecast using models such as WAM. Our results show however that the kurtosis and the freak wave activity strongly depend on the crest length of the waves, while a significant dependence on BFI is only seen for long-crested waves. Hence, our results imply that the proposed relationship, that kurtosis is proportional to BFI squared, does not hold for short-crested seas.

Our results imply a rather sharp parametric boundary between long- and short-crested seas for a characteristic crest length that is about ten characteristic wavelengths, $L_c \approx 10$. For long-crested seas we find a strong correlation between BFI and freak wave activity. For short-crested seas we find a much weaker (or hardly any) correlation between BFI and freak wave activity. In both cases there is a strong correlation between kurtosis and freak wave activity.

## 2. The simulation model

The present numerical simulations have been performed with the modified nonlinear Schrödinger equation of Trulsen & Dysthe (1996). This equation, the so-called BMNLS equation, allows for a slightly broader bandwidth than the MNLS equation of Dysthe (1979), and includes the same nonlinear effects as the MNLS equation. Throughout the rest of the paper, all lengths and times have been normalized by the peak wavenumber $k_p$ and angular frequency $\omega_p$ respectively.

The numerical solution of the BMNLS equation gives the complex amplitude, $B$, of the free waves from which the surface elevation and the amplitudes for the higher harmonics can be found consistently up to third order in wave steepness. The expression for $\eta$ has the form

$$\eta = \bar{\eta} + \tfrac{1}{2}(B\mathrm{e}^{\mathrm{i}\theta} + B_2\mathrm{e}^{2\mathrm{i}\theta} + B_3\mathrm{e}^{3\mathrm{i}\theta} + \cdots + \text{c.c.}), \tag{2.1}$$

where $\theta = x - t$. The zeroth harmonic, $\bar{\eta}$, and the complex amplitudes of the higher harmonics, $B_2, B_3, \ldots$, can be expressed in terms of $B$. However, our focus is how the free waves evolve due to nonlinear interactions, and not the static contribution from the nonlinearly bound waves. Therefore we only consider the first-harmonic contribution in (2.1).

To solve the BMNLS equation numerically, we use the method described by Lo & Mei (1985, 1987) with periodic boundary conditions in both horizontal directions. Additional details about the numerical implementation can be found in Socquet-Juglard *et al.* (2005).

We use a uniform grid of $n_x \times n_y = 256 \times 256$ points, which with our choice of discretization in the wave vector plane corresponds to $128 \times 128$ characteristic wavelengths. For the purely two-dimensional simulations we have used a two-dimensional version of the equation, with a computational domain of 16 384 characteristic wavelengths. In particular we have checked that the three-dimensional model gives results that converge to the two-dimensional model in the limit of long-crested waves.

In the following, we will consider wave fields initiated with both JONSWAP and Gaussian wave spectra. The Gaussian spectrum allows us to consider a wide range of different spectral widths, including very narrow-banded situations, while the JONSWAP spectrum describes a more realistic sea state.

The two-dimensional Gaussian wave spectrum for $\eta$ is in the form

$$F_G(\boldsymbol{k}) = \frac{\epsilon^2}{4\pi\sigma_x\sigma_y} \exp\left[-\left(\frac{(k_x-1)^2}{2\sigma_x^2} + \frac{k_y^2}{2\sigma_y^2}\right)\right]. \tag{2.2}$$

Here, $\boldsymbol{k} = (k_x, k_y)$ is the wave vector, $\epsilon$ is the average wave steepness and $\sigma_x$ and $\sigma_y$ are non-dimensional bandwidths in the $x$- and the $y$-direction, respectively. The wave vector is normalized such that the spectral peak is located at $\boldsymbol{k}_p = (1, 0)$.

In order to obtain the directional JONSWAP spectrum we use the linear dispersion relation for deep-water gravity waves to transform the JONSWAP frequency spectrum, $S_\omega(\omega)$, to a wavenumber spectrum, $S_k(k)$. We choose a directional distribution, $D(\phi)$, and define the wave spectrum as $F_J(\boldsymbol{k}) = (1/k)S_k(k)D(\phi)$. $S_k(k)$ is given as

$$S_k(k) = \frac{\alpha}{k^3} \exp\left[-\tfrac{5}{4}k^{-2}\right] \gamma^{\exp\left[-(\sqrt{k}-1)^2/(2\sigma^2)\right]}, \tag{2.3}$$

and the angular distribution is taken to be in the form

$$D(\phi) = \begin{cases} (1/\beta)\cos^2(\pi\phi/2\beta), & |\phi| \leqslant \beta, \\ 0, & \text{elsewhere.} \end{cases} \tag{2.4}$$

Here, $\gamma$ is the so-called peak enhancement coefficient and $\beta$ is a directional spreading coefficient, $\sigma$ has the standard values 0.07 for $k \leqslant 1$ and 0.09 for $k > 1$, and $\alpha$ is chosen such that the spectrum fulfils the normalization criterion

$$\int_{\boldsymbol{k}} F_J(\boldsymbol{k}) k \, \mathrm{d}k \, \mathrm{d}\phi = s^2 = \frac{\epsilon^2}{2}, \tag{2.5}$$

where $s$ is the standard deviation of the surface elevation, $s = \sqrt{\overline{\eta^2}}$.

The bandwidths $\Delta\omega$ and $\Delta k_y$ have been computed using the spectral half-width at half maximum. There exist several other possible definitions of the bandwidths that would yield slightly different values. For the Gaussian spectrum we could have used $\sigma_x$ and $\sigma_y$ as measures of bandwidth, while our definition above yields $\Delta k_y = \sigma_y\sqrt{2\ln 2}$.

We have performed a large number of simulations with different values of the parameters $\sigma_x$, $\sigma_y$, $\beta$ and $\gamma$ in the wave spectra given above. For the Gaussian spectrum, we have varied $\sigma_x$ in the range from 0.06 to 0.5 and $\sigma_y$ in the range from 0 to 0.5, both with step 0.02, i.e. $23 \times 26 = 598$ simulations for different combinations of $\sigma_x$ and $\sigma_y$. According to the definitions (1.1) and (1.2) this corresponds to BFI in the range from 0.4 to 2.9 and crest lengths from 1.7 characteristic wavelengths up to infinitely long-crested waves (two-dimensional waves). For the JONSWAP spectrum, the parameters $\gamma$ and $\beta$ control the bandwidths in the $x$- and $y$-directions, respectively. We have varied $\gamma$ from 1 to 6.8 with step 0.2, and $\beta$ from 0 to $\pi/2$ with step $\pi/60$, i.e. $31 \times 30 = 930$ simulations. This corresponds to BFI from 0.44 to 1.46 and crest lengths larger than 1.3 characteristic wavelengths.

The average steepness, $\epsilon$, is in all the simulations set to 0.1. However, in order to employ a narrow-banded model we truncate the spectra within $k_x^2 + k_y^2 \leqslant 1$ in the numerical solution. This means that some of the energy in the spectrum is left out, which implies that the simulated steepness in some cases is less than 0.1. Thus we consider the most energetic part of a sea state with steepness 0.1, but the average steepness measured from the numerical sea surface is less than 0.1. For the Gaussian initial spectrum the simulated steepness is in all cases larger than 0.093, and for most cases in practice equal to 0.1. For the JONSWAP spectrum, owing to its long tail, more of the energy is left out. For the broadest case ($\gamma = 1$, $\beta = \pi/2$) the simulated steepness is as small as 0.082, but for most of the cases it is above 0.09. Some trials with different initialization, such that the steepness is equal in all simulations, have been performed, and show very similar results to the ones presented here.

As a measure of the occurrence of large waves, we use the mean of the 1/1000 largest values of the upper envelope, $|B|$, of the free waves. We denote this quantity as $A_{1/1000}$. For example, if one assumes a Gaussian-distributed first-harmonic surface elevation, the upper envelope of the free waves will follow the Rayleigh distribution. Recall that $s$ denotes the standard deviation of the full wave field. Then for Rayleigh-distributed $|B|$ we find that $P(|B| > 3.7s) \approx 1/1000$. If we further account for bound-wave contributions, we can show that $P(E > 4.25s) \approx 1/1000$, where $E$ is the upper envelope of the full wave field (both free and bound waves) defined as $E = \bar{\eta} + |B| + |B_2| + |B_3| + \cdots$.

Given the Rayleigh distribution, one can show that the theoretical value of $A_{1/N}$ is

$$A_{1/N} = s\left[\sqrt{2\pi}\frac{N}{2}\mathrm{erfc}(\sqrt{\ln N}) + \sqrt{2\ln N}\right]. \tag{2.6}$$

If we set $N = 1000$ and $s = \epsilon/\sqrt{2} = 0.1/\sqrt{2}$ in (2.6), we obtain $A_{1/1000} = 0.28$. The deviation from this value can thus be considered a measure of the non-Gaussianity of the wave field. In the following we use the normalized value $A^*_{1/1000} = A_{1/1000}/A^R_{1/1000}$, where $A^R_{1/1000}$ is the theoretical Gaussian value calculated using the steepness corresponding to the truncated spectrum. In addition to $A^*_{1/1000}$, we also compute the kurtosis of the first-harmonic surface elevation from the formula

$$\text{kurtosis} = \frac{\overline{\eta^4}}{\overline{\eta^2}^2}. \tag{2.7}$$

## 3. Results

From each of the simulated realizations, we obtain time series of $A^*_{1/1000}$ and the kurtosis. Two sample time evolutions of $A^*_{1/1000}$ and the kurtosis are shown in

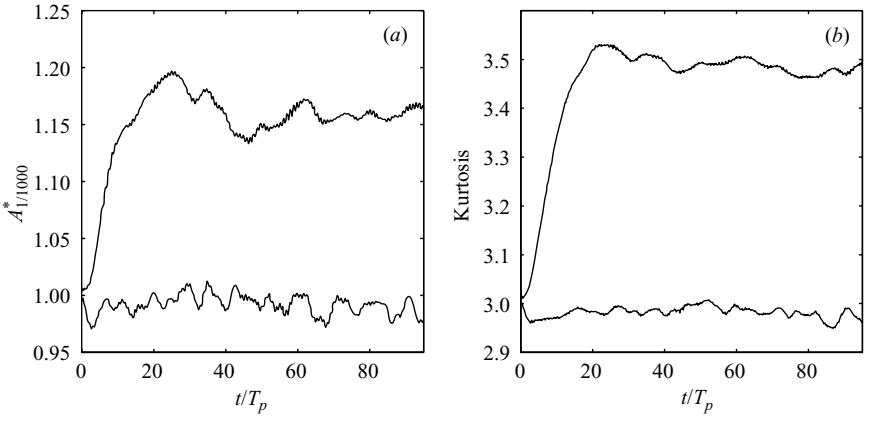


FIGURE 1. Typical examples of time evolutions of $A^*_{1/1000}$ and the kurtosis. The lower curves correspond to a realization that does not show significant deviations from Gaussian statistics. The upper curves show the evolution of a realization that produces non-Gaussian statistics.

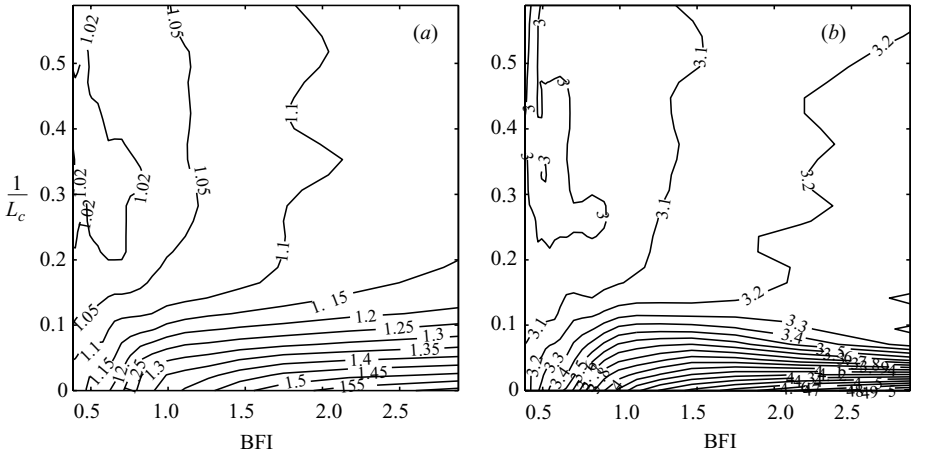


FIGURE 2. Contour plots of (*a*) the maximum of $A^*_{1/1000}$ during the simulated time series and (*b*) the corresponding kurtosis as a function of the BFI and crest length. Gaussian initial spectrum.

figure 1. The lower curves in figures 1(*a*) and 1(*b*) show a realization that more or less agrees with Gaussian statistics for all times. In this case, the evolution shows fluctuations around the Gaussian value. The upper curves correspond to a realization that produces non-Gaussian statistics. In such cases, we see a rapid transition from the Gaussian initial condition with uncorrelated phases into a non-Gaussian sea, which is probably more representative of a real nonlinear sea than the given initial condition. In this case, we must interpret the first part of the time evolution as a result of 'unrealistic' initial conditions.

In figures 2 and 3 we show how the generation of non-Gaussian statistics, and the larger probability of freak waves, depend on the BFI and the crest length of the initial spectrum. Figures 2 and 3 show the maximum value of $A^*_{1/1000}$ achieved during the simulation, and the corresponding kurtosis, for the Gaussian and JONSWAP initial spectra respectively. (Qualitatively similar results for the kurtosis have been

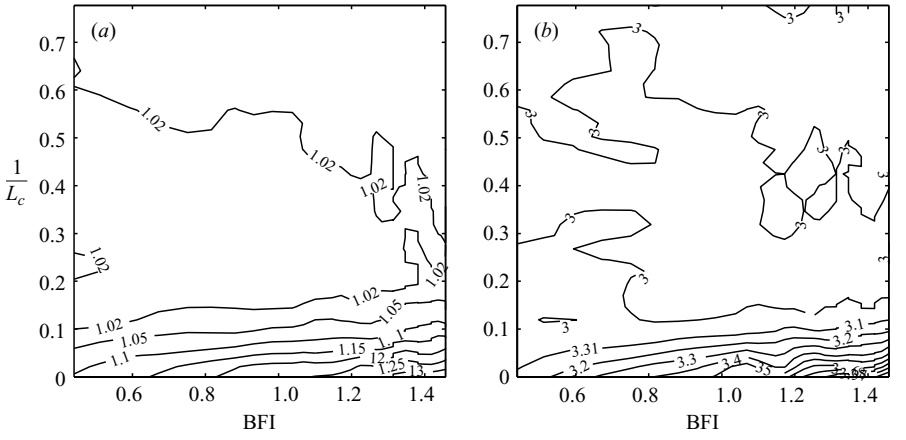


FIGURE 3. Same as figure 2, but for a JONSWAP initial spectrum.

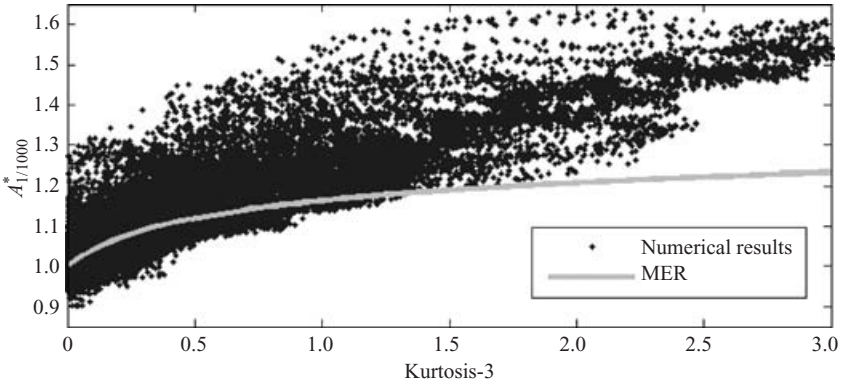


FIGURE 4. Relation between $A^*_{1/1000}$ and the kurtosis in the simulations with a Gaussian initial spectrum.

obtained using the cubic nonlinear Schrödinger equation by Miguel Onorato, personal communication).

We first note from figures 2 and 3, as well as from figure 1, that the kurtosis seems to be highly correlated with the occurrence of freak waves. This correlation is well known and is not surprising. Recently, Mori & Janssen (2006) used Edgeworth distributions to develop a correction to the Rayleigh distribution in the case where the kurtosis deviates from 3. This distribution has been named the modified Edgeworth–Rayleigh (MER) distribution. In order to see how the MER distribution agrees with our results, we have plotted in figure 4 the relation between $A^*_{1/1000}$ and the fourth-order cumulant of the surface elevation (the kurtosis minus 3) for all times in the simulated realizations (600 different times from 598 realizations with different initial spectra, approximately 360 000 data points) and compared it to the theoretical value of $A^*_{1/1000}$ using the MER distribution. Using the probability density function of the envelope given in equation (43) of Mori & Janssen (2006), we find

$$\langle A_{1/N}\rangle = \left(1-\frac{\kappa_4}{24}\right)\left[\frac{\alpha}{1+\frac{1}{24}\kappa_4\alpha^2(\alpha^2-4)}+N\sqrt{\frac{\pi}{2}}\mathrm{erfc}(\alpha/\sqrt{2})\right]+\frac{\kappa_4}{24}\frac{\alpha^3(\alpha^2-3)}{1+\frac{1}{24}\kappa_4\alpha^2(\alpha^2-4)}, \tag{3.1}$$

where $\alpha$ has the value such that

$$\frac{1}{N} = \mathrm{e}^{-\alpha^2/2}\left(1 + \tfrac{1}{24}\kappa_4\,\alpha^2(\alpha^2 - 4)\right). \tag{3.2}$$

We see that the MER distribution is in fairly good agreement with the numerical results for kurtosis less than about 4, but underestimates the probability of large waves when the kurtosis becomes larger. Our numerical results suggest that there is no dependence on the directionality of the waves in this result.

We now return to figures 2 and 3 and consider how the occurrence of large waves depends on BFI and the crest length of the initial spectra. Note that the spectra change during the simulation. Consequently, BFI and the crest length may be slightly different at the time of observation in figures 2 and 3 than for the initial spectrum. This effect is most apparent in cases with large BFI, where BFI decays during the first part of the simulation. The crest length is however nearly constant throughout the simulation.

The results for Gaussian and JONSWAP initial spectra are qualitatively similar. The occurrence of freak waves depends on both BFI and the crest length. Perhaps the most remarkable feature of figures 2 and 3 is that there seems to exist a well-defined boundary between short-crested and long-crested sea, at least for freak wave occurrence. This transition between short-crested and long-crested behaviour occurs when the crest length is about 10 times the characteristic wavelength, $L_c \approx 10$.

In the regions of figures 2 and 3 where $L_c$ is larger than 10, we observe large deviations from Gaussian statistics. Within this region the occurrence of freak waves shows a strong dependence on the crest length and BFI. For purely two-dimensional waves, we have the largest deviations from Gaussian statistics. In this region the probability of freak waves increases with increasing BFI.

In the short-crested region of figures 2 and 3 ($L_c$ less than 10), we observe nearly Gaussian properties. For a Gaussian initial spectrum the freak wave probability slightly exceeds Gaussian theory when BFI becomes large for short-crested waves. For our choice of parameters in the JONSWAP spectrum, we are unable to detect any correlation between BFI and the probability of freak waves for short-crested waves.

## 4. Discussion

We have shown that the probability of large waves in a given sea state depends on both the spectral width in the direction of the main wave propagation (or alternatively the group length or BFI) and the spectral width in the direction perpendicular to the direction of wave propagation (or alternatively the crest length). One should consider both of these parameters in order to correctly predict the probability of freak waves from knowledge of the wave spectrum.

Theoretical and experimental works (Stansberg 1994; Onorato *et al.* 2002; Socquet-Juglard *et al.* 2005; Waseda 2006) have previously suggested that there is a qualitative difference in the statistics of large waves for long-crested and short-crested seas. Our results suggest that there is a sharp qualitative transition between these two regimes for a crest length of approximately ten times the characteristic wavelength. The sharp transition is supported by the experimental results of Waseda (2006).

When the crest length is shorter than the threshold, we see noticeable deviation from Gaussian statistics only for very large BFI. Sufficiently large BFI was only achieved for the Gaussian initial spectrum, and not for the JONSWAP initial spectrum with our choice of peak enhancement factor $\gamma \leqslant 6.8$.

When the crest length is longer than the threshold, we observe significantly more freak waves than predicted by Gaussian statistics. For the long-crested sea, the freak wave probability increases with increasing BFI and increasing crest length.

We have confirmed that there is a strong correlation between the likelihood of freak waves and kurtosis, both for short-crested and long-crested seas. This is in qualitative agreement with results due to Mori & Janssen (2006) based on Edgeworth distributions.

It has been suggested that the kurtosis can be found from knowledge of the spectrum (Janssen 2003; Onorato *et al.* 2005*b*; Mori & Janssen 2006). This would enable a direct prediction of freak wave probability from the estimate of BFI from a spectral wave forecast. Specifically, they suggested that the kurtosis is proportional to BFI squared. Our results do not support such a correlation except for long-crested seas.

If realistic sea states have crest lengths shorter than ten wavelengths, we anticipate that freak waves in these sea states belong to the Tayfun distribution independently of the group length. If crest lengths longer than ten do occur, we anticipate that freak waves occur more frequently. Hence, rather than using BFI as the only indicator, better prediction of freak wave activity can be achieved by the simultaneous consideration of crest length and BFI. Observations of directional spreading of hurricane generated waves by Young (2006) suggest crest lengths well below 10. We estimate an upper bound for the crest lengths in his observations to be $L_c \approx 7$.

Throughout our work we have considered a fixed overall steepness corresponding to a wind sea close to saturation. It remains to investigate variable overall steepness as a third parameter in addition to the group and crest lengths. BFI is the product of steepness and group length, so BFI can have significance beyond what has been revealed in our present investigation.

We would like to acknowledge the several useful comments by one of the referees.

## REFERENCES

Alber, I. E. 1978 The effects of randomness on the stability of two-dimensional surface wavetrains. *Proc. R. Soc. Lond.* A **363**, 525–546.

Benjamin, T. B. 1967 Instability of periodic wavetrains in nonlinear dispersive systems. *Proc. R. Soc. Lond.* A **299**, 59–75.

Clamond, D. & Grue, J. 2002 Interaction beween envelope solitons as a model for freak wave formations. Part i: Long time interaction. *C. R. Méc.* **330**, 575–580.

Crawford, D. R., Saffman, P. G. & Yuen, H. C. 1980 Evolution of a random inhomogeneous field of nonlinear deep-water gravity waves. *Wave Motion* **2**, 1–16.

Dysthe, K. B. 1979 Note on a modification to the nonlinear Schrödinger equation for application to deep water waves. *Proc. R. Soc. Lond.* A **369**, 105–114.

Dysthe, K. B. & Trulsen, K. 1999 Note on breather type solutions of the NLS as models for freak-waves. *Physica Scripta* **T82**, 48–52.

Janssen, P. A. E. M. 2003 Nonlinear four-wave interactions and freak waves. *J. Phys. Oceanogr.* **33**, 863–884.

Lo, E. & Mei, C. C. 1985 A numerical study of water-wave modulation based on a higher-order nonlinear Schrödinger equation. *J. Fluid Mech.* **150**, 395–416.

Lo, E. Y. & Mei, C. C. 1987 Slow evolution of nonlinear deep water waves in two horizontal directions: A numerical study. *Wave Motion* **9**, 245–259.

McLean, J. W., Ma, Y. C., Martin, D. U., Saffman, P. G. & Yuen, H. C. 1981 Three-dimensional instability of finite-amplitude water waves. *Phys. Rev. Lett.* **46**, 817–820.

Mori, N. & Janssen, P. A. E. M. 2006 On kurtosis and occurrence probability of freak waves. *J. Phys. Oceanogr.* **36**, 1471–1483.

Onorato, M., Osborne, A. R. & Serio, M. 2002 Extreme wave events in directional, random oceanic sea states. *Phys. Fluids* **14**, L25–L28.

Onorato, M., Osborne, A. R. & Serio, M. 2005*a* Modulational instability and non-Gaussian statistics in experimental random water-wave trains. *Phys. Fluids* **17**, 1–4.

Onorato, M., Osborne, A. R. & Serio, M. 2005*b* On deviations from Gaussian statistics for surface gravity waves. In *'Aha Huliko'a Rogue Waves 2005*, pp. 79–83.

Onorato, M., Osborne, A. R. & Serio, M. 2006 Modulational instability in crossing sea states: A possible mechanism for the formation of freak waves. *Phys. Rev. Lett*. **96**, 1–4.

Onorato, M., Osborne, A. R., Serio, M. & Bertone, S. 2001 Freak waves in random oceanic sea states. *Phys. Rev. Lett*. **86**, 5831–5834.

Onorato, M., Osborne, A. R., Serio, M., Cavaleri, L., Brandini, C. & Stansberg, C. T. 2004 Observation of strongly non-Gaussian statistics for random sea surface gravity waves in wave flume experiments. *Phys. Rev*. E **70**, 1–4.

Osborne, A. R., Onorato, M. & Serio, M. 2000 The nonlinear dynamics of rogue waves and holes in deep-water gravity wave trains. *Phys. Lett*. A **275**, 386–393.

Socquet-Juglard, H., Dysthe, K., Trulsen, K., Krogstad, H. E. & Liu, J. 2005 Probability distributions of surface gravity waves during spectral changes. *J. Fluid Mech*. **542**, 195–216.

Stansberg, C. T. 1994 Effects from directionality and spectral bandwidth on non-linear spatial modulations of deep-water surface gravity wave trains. In *Proc. 24th Intl Conf. on Coastal Engineering, Kobe, Japan, October 23–28, 1994*, pp. 579–593. ASCE.

Tayfun, M. A. 1980 Narrow-band nonlinear sea waves. *J. Geophys. Res*. **85**, 1548–1552.

Trulsen, K. & Dysthe, K. B. 1996 A modified nonlinear Schrödinger equation for broader bandwidth gravity waves on deep water. *Wave Motion* **24**, 281–289.

Waseda, T 2006 Impact of directionality on the extreme wave occurrence in a discrete random wave system. In *9th Intl Workshop on Wave Hindcasting and Forecasting, Victoria, B.C., Canada, September 24–29, 2006*.

Young, I. R. 2006 Directional spectra of hurricane wind waves. *J. Geophys. Res*. **111** (C08020).